Journal of Engineering and Technology for Industrial Applications

ITEGAM-JETIA

Manaus, v.11n.55, p. 11-19. September/October, 2025.
DOI: https://doi.org/10.5935/jetia.v11i55.1836.

ISSN ONLINE: 2447-0228

RESEARCH ARTICLE OPEN ACCESS

EXTENDED KALMAN FILTER ESTIMATOR AND MAMDANI FUZZY LOGIC CONTROLLER FOR SENSORLESS DC MOTOR SPEED CONTROL

Hadjer Abderrezek[1], Ameur Aissa[2]

[1,2] Electrical Engeneering Institute – Laghouat, Algeria.

[1]https://orcid.org/0009-0003-0246-0756, [2]https://orcid.org/0000-0001-5332-7697.

Email: h.abderrezek@lagh-univ.dz, a.ameur@ lagh-univ.dz.

ARTICLE INFO

Article History
Received: April 10, 2025
Revised: May 20, 2025
Accepted: September 15, 2025
Published: September 30, 2025

Keywords:
DC motor,
Mamdani Fuzzy Logic,
Extended Kalman Filter,
PI,
Sensorless Speed Control.

ABSTRACT

This article proposes a sensorless speed control method for DC motors that employs an extended Kalman filter (EKF) estimator and a Mamdani fuzzy logic controller (FLC). In many industries, expensive measurement systems are typically necessary for effective control and monitoring. However, this sensorless approach offers a cost-effective alternative that also enhances system reliability and robustness. The EKF estimates motor speed based solely on the armature current. Concurrently, the FLC assists in mitigating motor parameter variations and load torque nonlinearity in closed-loop speed control for various speed references. A comparative analysis of the performance of the EKF-based FLC with an FLC-based PI controller reveals that the former surpasses the latter in terms of time-domain specifications and absolute error performance indices. The integration of sensorless speed control techniques in DC motors has garnered significant attention due to its cost effectiveness and efficiency. This paper explores the use of an Extended Kalman Filter (EKF) estimator in conjunction with a Fuzzy Logic Controller (FLC) to improve the speed control performance of DC motors. The proposed system is implemented in MATLAB/Simulink, and a prototype model of a sensorless speed-controlled DC motor has been developed to validate this innovative technique.

I. INTRODUCTION

Electromechanical devices known as DC machines are capable of converting electrical energy into mechanical energy. These machines are utilized in a variety of applications, including industrial, transportation, and automotive sectors. Their operational mechanism entails the generation of a magnetic field by an electric current that flows within the windings of the inductor. This magnetic field subsequently interacts with the magnetic field of the rotor, thereby producing a driving torque that results in the rotation of the machine. The merits of DC machines are manifold, including but not limited to the following: variable speed, good speed and torque control, high reliability, and long life. They are also characterized by ease of control and maintenance [1].

The utilization of direct current (DC) motor drives has become pervasive in a multitude of applications, including rolling mills, paper mills, robots, electric vehicles, and analogous systems, where the ability to modulate speed and maintain constant or low speed torque is paramount [2]. Contemporary methodologies for regulating the velocity of electrical machines are manifold. A prominent approach entails the implementation of a PID controller, operating in conjunction with LabVIEW software, to ascertain motor speed through sensor measurement [3]. Furthermore, a comprehensive investigation into various optimization algorithms has emerged, aiming to refine the PID parameters [4]. Other studies have examined pulse width modulation (PWM) controlled BLDC motor drives [5].

In these methodologies, researchers employed a speed sensor or tachometer generator to gauge velocity. This approach, however, led to an escalation in hardware complexity and cost, accompanied by a reduction in reliability [6]. To enhance speed control effectively, a closed-loop system was necessitated, necessitating the utilization of known or feedbacked engine state variables [7]. This requisite system necessitated the integration of multiple mechanical sensors to measure all system state variables, thereby augmenting system size,

complexity, and cost while concomitantly diminishing robustness and reliability[8]. To address these issues by minimizing sensors and system complexity, researchers focused on sensorless control strategies with intelligent control for optimal response [9].

Sensorless control techniques rely on an observer/estimator comprising relevant electrical signals to estimate motor speed [10].Standard state estimation techniques include the following: sliding mode observer, model reference adaptive system, Luenberger observer, Kalman filter (KF), and extended Kalman filter (EKF) [11].The KF is a linear-time state estimator that is suitable for linear systems with known parameters; however, its performance degrades for nonlinear systems [12].The EKF is often used to overcome nonlinearity problems in practical applications [13]. The efficacy of sensorless speed control is contingent upon the effectiveness of the estimation algorithm employed [14]. The development of an optimal sensorless speed controller necessitates a comprehensive understanding of the motor's mathematical model and the environmental disturbances it experiences. However, in practice, such systems are frequently nonlinear and subject to uncertain disturbances and variations in motor parameters [15].

Fuzzy logic control (FLC) is a computational method that is based on fuzzy set theory. It addresses approximate reasoning as opposed to fixed and precise reasoning [16]. FLC allows for more human-like reasoning in decision making and is especially helpful in systems where ambiguity and imprecision are common [17]. Fuzzy sets allow degrees of membership ranging from 0 to 1. This is in contrast to classical sets where elements have binary membership (either belonging or not belonging) [18]. This characteristic enables the representation of concepts that are inherently vague or indefinable, such as "warm" or "fast"[19]. Fuzzy logic control provides a robust framework for managing complex systems in uncertain environments [20]. Its capacity to integrate human-like reasoning renders it indispensable in numerous domains, enhancing automation and decision-making processes while preserving flexibility in the face of novel challenges.

In this study, we used a system that combined fuzzy logic control (FLC) and the EKF algorithm to improve how quickly the system responded and how accurately it tracked speed, even when the reference speed, motor parameters, and load torque were different.We were able to estimate the speed of the DC motor shaft using an EKF observer, which was based exclusively on the sensed armature current.The estimated shaft speed was then fed back to the FLC, thereby generating a control signal for closed-loop sensorless speed control of the DC motor.The paper is organised as follows: Section 2 presents the mathematical model of a DC motor; Section 3 introduces the EKF state estimation algorithm; Section 4 discusses the implementation of EKF with FLC; and Sections 5 and 6 present the results and concluding remarks.

II. DC MOTOR MODELING

A mathematical model is needed to work out the state of a DC motor. The model has two main equations, one for the mechanical and one for the electrical parts of the motor [21].

The dynamics of the separately excited DC motor and its load are represented by the following set of differential equations with constant coefficients:

$$v(t) = e_a(t) + R_a i_a(t) + L_a \frac{d}{dt} i_a(t) \tag{1}$$

Where $e_a(t)$ is the back emf, $v(t)$ is the armature supply voltage, R_a is the armature resistance, L_a is the armature self-inductance caused by the armature flux, and $i_a(t)$ is the armature current.

The back emf $e_a(t)$ is given by the equation

$$e_a(t) = K.\varphi.\omega \tag{2}$$

The electromagnetic torque T_e is calculated using the following formula:

$$T_e = K.\varphi.I_a \tag{3}$$

The electromagnetic torque developed within the machine is counterbalanced by the load torque, friction, and inertia. This can be expressed as follows:

$$T_e = J\frac{d\omega_m}{dt} + B_m\omega_m + T_L \tag{4}$$

Where ω_m is the motor speed, J is the moment of inertia of the motor and load, B_m is the viscous damping coefficient and T_L is the load torque.

Equations (1) and (4) can be used to implement the state space model. Two state variables make up the model : motor speed (ω_m) and armature current (i_a). In the time domain, the state space model is represented as

$$\begin{bmatrix} \dot{i_a} \\ \dot{\omega_m} \end{bmatrix} = \begin{bmatrix} \frac{-R_a}{L_a} & \frac{-K_b}{L_a} \\ \frac{K_t}{J} & \frac{-B_m}{J} \end{bmatrix} \begin{bmatrix} i_a \\ \omega_m \end{bmatrix} + \begin{bmatrix} \frac{1}{L} & 0 \\ 0 & \frac{-1}{J} \end{bmatrix} \begin{bmatrix} v \\ T_L \end{bmatrix} \tag{5}$$

Table 1 shows the model parameters, their definitions, and the values of the engine for this work.

Table 1: The DC Motor parameters and specifications.

Description	Specification
L_a : armature inductance	5.2 e-3(H)
R_a : armature resistance	2 (ohm)
J : moment of inertia	1.5 e-4 (kg.m^2)
B_m : Coefficient of viscous friction	1 e-3
K_t : Torque constant	0.1 (N.m/A)

Source: Authors, (2025).

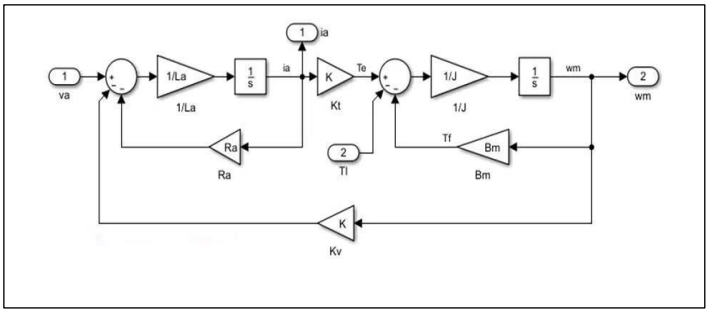

Figure 1: DC Machine Block Diagram.
Source: Authors, (2025).

Following the substitution of the values from Table 1 in (1) and (2), and the selection of a sampling time (Ts) of 1 millisecond, the DC motor model is converted to the discrete form using a MATLAB function. The following equations can be used to express the discrete-time model of the system:

$$x_{k+1} = A_d\, x_k + B_d\, u_k + v_k \tag{6}$$
$$y_k = C_d\, x_k + w_k \tag{7}$$

The process noise and measurement noise are represented by the variables : state variable $x[i_a \quad \omega_m]^T$, input vector $u = [i_a \quad \omega_m]^T$, and the output vector $y = [i_a \quad 0]^T$ in the equation above. Q and R represent the mean zero covariance, respectively.
The discretized matrix coefficients A_d, B_d and C_d at sampling time T_s can be written as :

$$A_d = I + AT_s = \begin{bmatrix} 1 & 0{,}005 \\ -0{,}007 & 0{,}9828 \end{bmatrix} \tag{8}$$
$$B_d = B.T_s = \begin{bmatrix} -0.016 & 0 \\ 0 & 0{,}0067 \end{bmatrix} \tag{9}$$
$$C_d = C = [0 \quad 1] \tag{10}$$

We determine that this system is controllable and observable using the Kalman controllability and observability test, wich suggests that we can construct a controller and observer. The detailed performance of the EKF estimator and observer is given in the next section.

III. EXTENDED KALMAN FILTER OBSERVER

Based on this data, the observer estimates the motor speed (ω_m) using the state space model created in Section 2. The EKF observer calculates the best possible state from a noisy state by applying iterative mathematical formulas. Since the load torque in the system is nonlinear (the DC motor model becomes nonlinear when θ is calculated using (ω_m), the KF is irrelevant for nonlinear systems. Consequently, EKF is used to get around the nonlinear problem KF. The extended version of KF, or EKF, estimates the state from noisy measured data by using a first-order Taylor series approximation of the nonlinear dynamic function. State prediction and state correction are the two primary processes of the EKF.

In the prediction phase, a dynamical model of the system with process noise covariance Q is employed. In the correction stage, measured data and Kalman gain (K) adjust the expected state.Accurate initial values of all the covariance matrices Q, R, and P are required to implement EKF; otherwise, the system may diverge and become unstable.The covariance can be obtained by studying the stochastic properties of the associated noise. These are obtained here both naturally and with the help of [22]. The mathematical steps for the EKF are listed below.The prediction step is :

$$\hat{x}_{k+1/k} = f(\hat{x}_k, u_k) \tag{12}$$
$$P_{k+1/k} = A_d P_k \grave{A}_d + Q \tag{13}$$

Where the estimated state of x_k is denoted by $\hat{x}_k$.
The rectification step is

$$K_{K+1} = P_{K+1/K}\, \grave{C}_d \left(C_d P_{K+\frac{1}{K}} \grave{C}_d + R \right)^{-1} \tag{14}$$
$$\hat{x}_{k+1} = \hat{x}_{k+1/k} + K_{k+1}(y_{k+1} - C_d \hat{x}_{k+1/k}) \tag{15}$$
$$P_{k+1} = P_{k+1/k}\ \ (I - K_{k+1}\, C_d) \tag{16}$$

I is the identity, and K_{k+1} is the Kalman gain at *(k+1)* time indices.
Equations (12) through (16) represent a single cycle of the EKF algorithm.

IV. RESULTS AND DISCUSSIONS

This section delineates two potential designs for controllers that can be utilised in the context of DC motor speed control. The configuration of the system under consideration is illustrated in Figure 1.

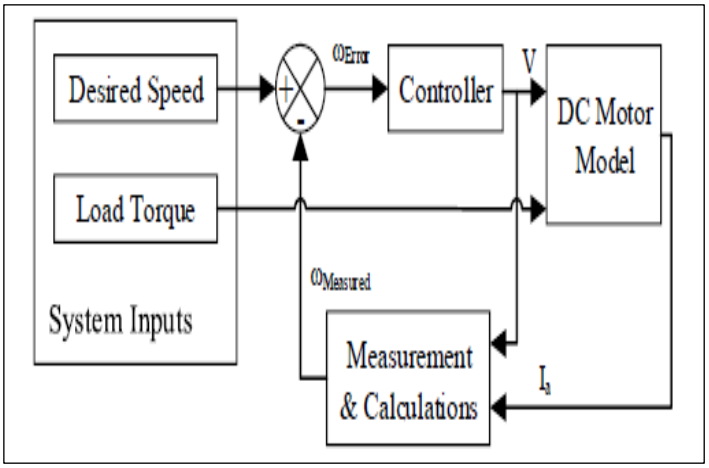

Figure 2: A DC motor with a controller and speed feedback.
Source: Authors, (2025).

Most processes must be controlled at their predetermined points because they cannot operate with an offset. To do this, additional intelligence must be added to the proportional controller, which is accomplished by adding an integral action to the original proportional controller. As a result, the controller becomes an integral proportional controller. The symmetric optimal criterion is used in the initial design of the proportional integral (PI) speed controller [8], This makes the difference between the measured motor speed (w) and the reference speed (ω_{ref}) as small as possible.

The PI controller continuously adjusts its output while an error is present and stops adjusting its output when the error is corrected or zeroed.

- Integration eliminates offset or inaccuracy, but it can occasionally exacerbate transient response.
- With a PI controller, the controller's output is adjusted in proportion to the integral of the error.

Where K_i is the integral gain of the PI controller, the PI controller can be expressed mathematically as follows.

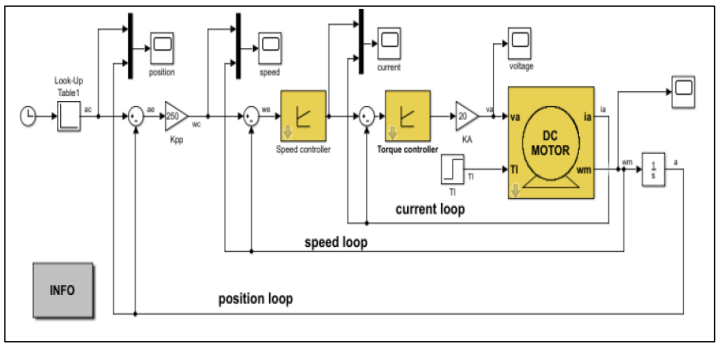

Figure 3: Cascade Position Control Diagram of DC Motor.
Source: Authors, (2025).

In this section, we introduced the fuzzy controller for adjusting the speed of a DC motor, namely the Mamdani type controller. The control law for a fuzzy speed controller is a function of the speed error (e) and its derivative (de) such that $C_{em}^{*}(t) = f(e, de)$, This allows the set of related decision rules to give the necessary variation of the (dC_{nem}) command. In simple cases, this variation of the command is obtained by reading a decision table that has been defined offline.
The most general form of this control law is

$$C_{em}^{*}(t) = C_{em}^{*}(t-1) + K_{du} dC_{nem} \tag{17}$$

With : C_{em}^{*} : Reference electromagnetic torque.
The error and the error derivative are adapted as follows:

$$e = K_e \tag{18}$$

$$de = K\, d_e\, de_n \tag{19}$$

The primary focus of this study is the speed controller within a linearization control by linearization input-output of the DC machine. The reference speed can be controlled by an external operator, and the output quantity of this cruise control is the electromechanical torque. The two inputs of the fuzzy controller are the speed error and its variation.

The speed error, denoted by e, is defined by the following equation:

$$e = \Delta\omega = \omega_{ref} - \omega_r \tag{20}$$

The variation of the velocity error denoted Δe is defined by the following equation :

$$\Delta e = e(t + \Delta t) - e(t) = e(k + 1) - e(k) \quad (21)$$

As illustrated in Table II, the FLC rules base is presented in sequential order. These guidelines are designed to develop an FLC controller by simulating the operation of a traditional PI controller.

The membership functions are of the triangular and trapezoidal type on the boundaries. The range of interest of the input variables is subdivided into three classes for the error "e" and the derivative "de/dt" and the output variable "S".

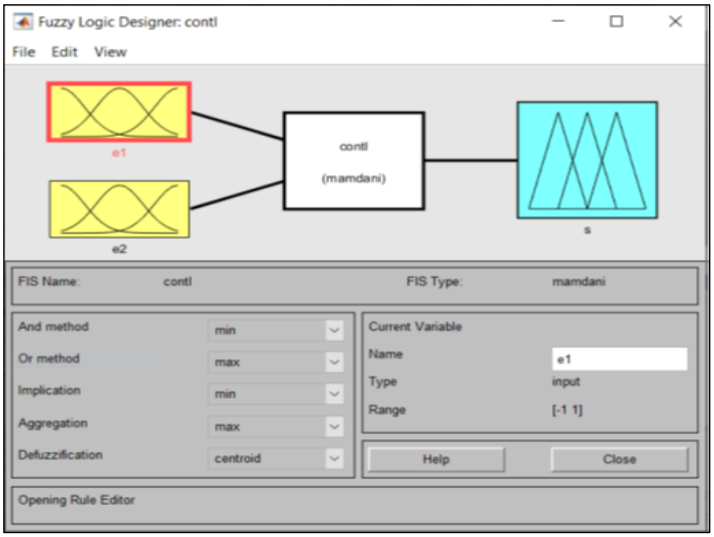

Figure 4: The global structure (input, output, the categorization of operators).
Source: Authors, (2025).

This interface is employed to delineate the ranges of inputs and outputs, thereby constraining the behavior of the fuzzy block. The following is a list of the designated ranges: NL is Negative Large; NM is Negative Medium; NS is Negative Small; ZO is Zero; PS is Positive Small; PM is Positive Medium; and PL is Positive Large.

Table 2: FLC Rule base.

Control Output UPI		Error (e)						
		NL	*NM*	*NS*	*ZO*	*PS*	*PM*	*PL*
Rate of Change of Error (ce)	*PL*	ZO	PS	PL	PL	PL	PL	PL
	PM	NS	ZO	PS	PM	PL	PL	PL
	PS	NL	NS	ZO	PS	PM	PL	PL
	ZO	NL	NM	NS	ZO	PS	PM	PL
	NS	NL	NL	NM	NS	ZO	PS	PL
	NM	NL	NL	NL	NM	NS	ZO	PS
	NL	NL	NL	NL	NL	NL	NS	ZO

Source: Authors, (2025).

The output is then determined according to the respective weights of the different input laws. Indeed, the laws overlap, and therefore an output value is a function of several input laws on the same quantity. To illustrate the tuning performance through fuzzy logic, we simulated the block diagram of the speed control of a direct current motor, which is represented by figure5.
The values of the regulator's gains are chosen after several adjustment tests.

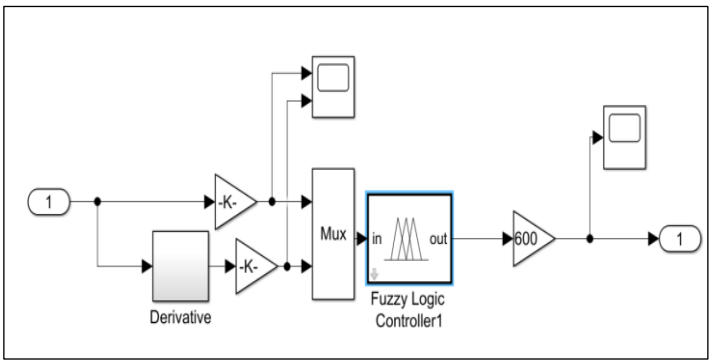

Figure 5: Diagram of speed control by fuzzy logic.
Source: Authors, (2025).

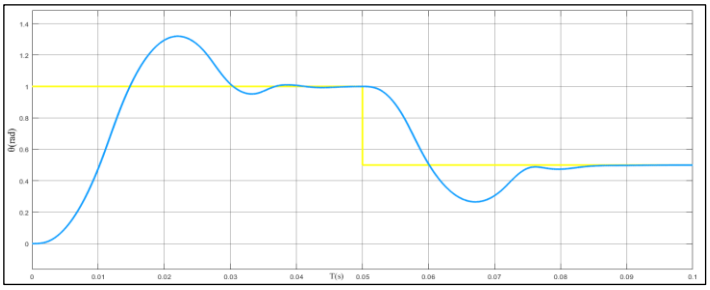

(a) DC Motor position.

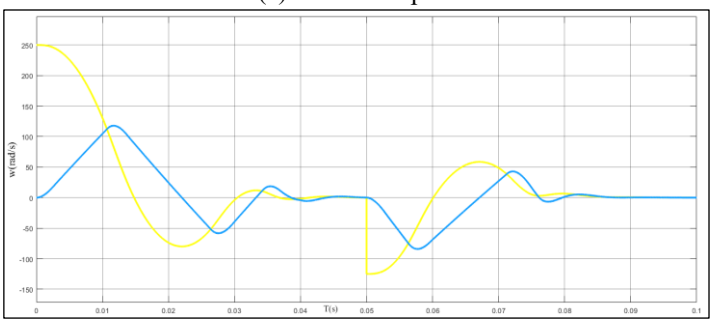

(b) *Mamdani FLC Controller*

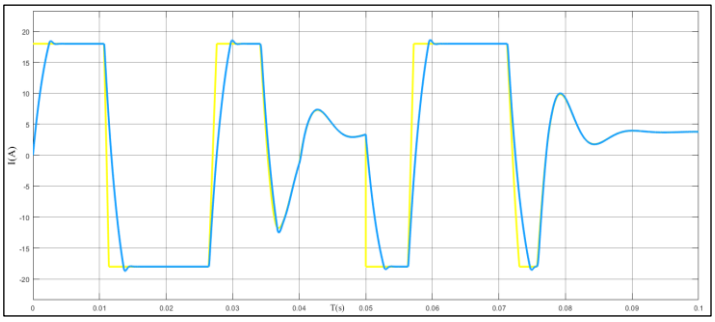

(c) DC motor current

Figure 6: DC motor speed after reversing the rotation direction.
Source: Authors, (2025).

After loading the regulator into the fuzzy block of Simulink, the system was simulated, and the following response was obtained.

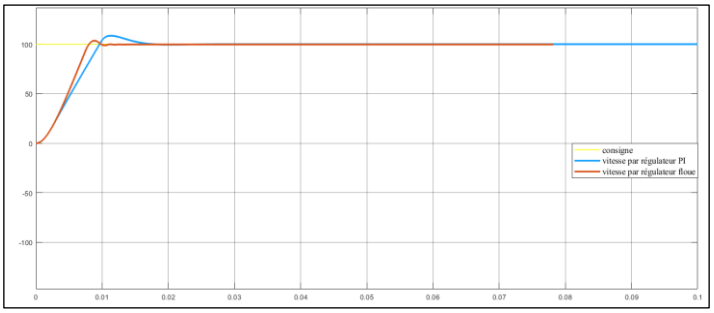

Figure 7: The difference in speed between the fuzzy regulator and the PI regulator with load.
Source: Authors, (2025).

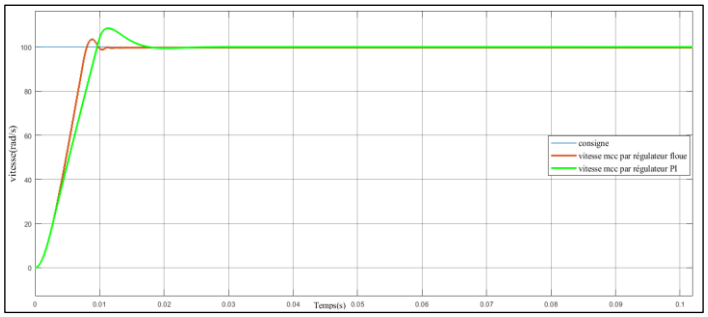

Figure 8: The DC Motor speed by fuzzy regulator and PI regulator without load.
Source: Authors, (2025).

As demonstrated in Figure 7, a clear distinction emerges in the rate of convergence between the fuzzy regulator and the PI regulator when subjected to an external load. In Figure 8, the speed of a DC motor is exhibited under two distinct regulatory conditions : one scenario involves the implementation of a fuzzy regulator, while the other scenario utilizes a PI regulator in the absence of an external load.

The results obtained indicate that the index response of the PI controller and LF exhibits an overshoot. The PI regulator provides less satisfactory responses in terms of speed, with increased overshoot, whereas the response time of the fuzzy controller is faster and minimizes overshoot. Additionally, the overshoot tends to be high if the gain is increased. In consideration of the findings regarding accuracy, rise time, response time, and system stability, it is evident that the judicious selection of membership functions enables the fuzzy controller to demonstrate superior performance in comparison to the PI controller.
The implementation of the Kalman filter in a particular problem context necessitates the following sequence of steps:

- Selection of the state variable of the system under study and establishment of the mathematical model in accordance with the equations.
- Estimation of the initial conditions.
- Calculation of the filter's recursive equations.
- Verification of the application's assumptions through examination of the residuals and critical evaluation of the results.

The system under consideration comprises two blocks: the controller block and the DC motor block. The controller block contains PWM generators, FLC, and EKF observers. To estimate the states (speed and current) of the DC motor, the EKF code was written in the EKF estimator block using the MATLAB code generator block.The difference between the estimated and reference speeds creates the error signal. The FLC controller receives the generated error and change in error as inputs and uses these to create the duty cycle and pulse with needed to regulate the speed of the DC motor.

The subsequent section presents the results of the state estimation simulation of the DC Motor using the adaptive extended Kalman filter (by adjusting the elements of the Q and R matrices). That is to say, the results are calculated from the state and measurement noises whose variances are provided.

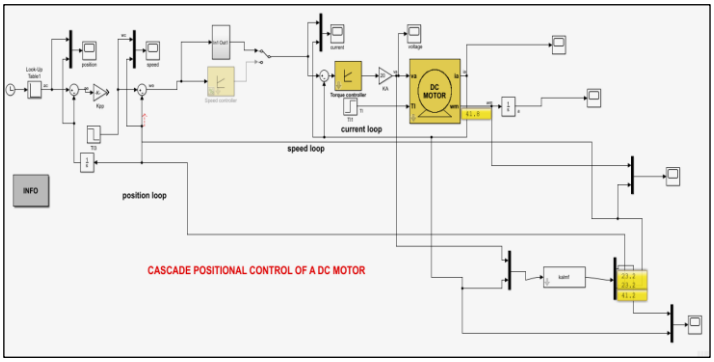

Figure 9: Diagram showing the speed sensorless control of an EKF DC motor with an FLC.
Source: Authors, (2025).

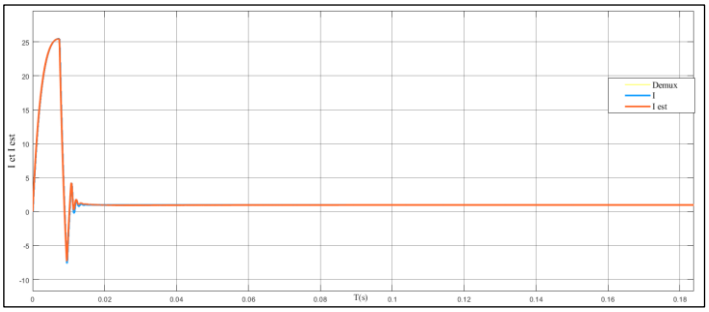

Figure 10: DC Motor estimation current of an EKF with FLC.
Source: Authors, (2025).

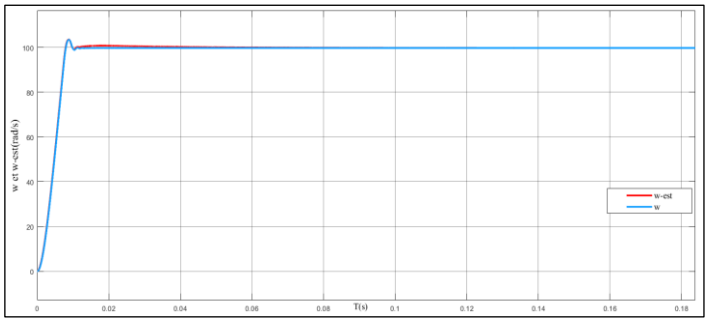

Figure 11: DC Motor estimation speed of an EKF with FLC.
Source: Authors, (2025).

As illustrated in Figure 10, the simulation diagram depicts the speed sensorless control of a DC motor equipped with an EKF and an FLC. In Figure 11, the estimation of the current of a direct current (DC) motor of an extended Kalman filter (EKF) with a finite-length controller (FLC) is demonstrated.

This paper proposes a sensorless closed-loop speed control strategy for a direct current (DC) motor, implemented through the integration of an extended Kalman filter (EKF) with a fuzzy logic controller (FLC). The efficacy of this approach is demonstrated through numerical illustrations, specifically in Figures 10 and 11, which depict the closed-loop performance of speed and current control for the EKF with FLC in the absence of a load.

The present study has demonstrated that the induced current of the direct current (DC) motor of the EKF with the fuzzy logic control (FLC) has exhibited minor estimation inaccuracy. The speed errors are delineated as the discrepancy between the reference speed and the actual speed obtained by the FLC controller. It can be ascertained that the EKF rapidly estimates the motor speed without the necessity of a speed sensor. The EKF with the FLC controller exhibits superior proficiency in tracking the reference speed.

V. CONCLUSIONS

In this paper, we presented a nonlinear state observer (extended Kalman filter) to estimate the speed and current of a direct current motor controlled by both Mamdani-RLF and PI control techniques. The elimination of physical sensors reduces system complexity and cost, making sensorless speed control an attractive solution for DC motor applications. The EKF estimator estimates the motor speed based on available measurements, compensating for the lack of direct speed sensors. The EKF estimation method has been shown to be robust, even in the presence of noise and uncertainties.

The findings from the simulation demonstrate the efficacy of the extended Kalman filter, as evidenced by its ability to generate a minimal estimation error across a range of rotational speeds (high speeds, low speeds) and its resistance to variations in load.The FLC controller is engineered to regulate motor speed based on the estimated values provided by the EKF estimator.The FLC incorporates adaptive learning capabilities, facilitating precise control adjustments in real time. The combination of the EKF estimator and the FLC controller has been shown to yield a synergistic effect, thereby enhancing the overall speed control performance of the DC motor system.

The EKF provides accurate speed estimation, while the FLC optimally adjusts control signals for improved dynamic response. It can be concluded that the integration of an EKF estimator with a FLC controller represents a promising avenue for advancing sensorless speed control capabilities in DC motors. This integrated approach offers enhanced accuracy, robustness, and efficiency in regulating motor speeds while minimizing hardware requirements and costs.

VI. AUTHOR'S CONTRIBUTION

Conceptualization: Hadjer Abderrezek and Ameur Aissa.
Methodology: Hadjer Abderrezek and Ameur Aissa.
Investigation: Hadjer Abderrezek and Ameur Aissa.
Discussion of results: Hadjer Abderrezek and Ameur Aissa.
Writing – Original Draft: Hadjer Abderrezek and Ameur Aissa.
Writing – Review and Editing: Hadjer Abderrezek and Ameur Aissa.
Resources: Hadjer Abderrezek and Ameur Aissa.
Supervision: Hadjer Abderrezek and Ameur Aissa.
Approval of the final text: Hadjer Abderrezek and Ameur Aissa.

VIII. REFERENCES

[1] N. Mohsenizadeh, S. Darbha, and S. P. Bhattacharyya, "Synthesis of PID controllers with guaranteed non-overshooting transient response," Proceedings of the 50th IEEE Conference on Decision and Control and European Control Conference, Orlando, FL, pp. 447–452, Dec. 2011.

[2] B. I. Saeed and B. Mehrdadi, "Zero overshoot and fast transient response using a fuzzy logic controller," Proceedings of the 17th International Conference on Automation and Computing, Huddersfield ,pp. 116–120,Sep. 2011.

[3] J. Chaoraingern, A. Numsomran, T. Suesut, T. Trisuwannawat, and V. Tipsuwanporn, "PID controller design using characteristic ratio assignment with an experimental application to temperature control," International Journal of Innovative Computing, Information and Control, vol. 8, no. 8, pp. 5801–5814, Aug. 2012.

[4] U. Kabir, M. F. Hamza, A. Haruna, and G. S. Shehu, "Performance analysis of PID, PD and fuzzy controllers for position control of 3-DOF robot manipulator," arXiv preprint arXiv:1910.12076, Oct. 2019.

[5] M. Nassim and A. Abdelkader, "Speed control of DC motor using fuzzy PID controller," arXiv preprint arXiv:2108.05450, Aug. 2021.

[6] "Strategies to avoid overshoot in PID Control," PID-tuner.com. [Online]. Available: https://www.pid-tuner.com/overshoot-in-pid-control/. Accessed: Mar. 6, 2025.

[7] "Proportional Integral (PI) Control," APMonitor. [Online]. Available: https://apmonitor.com/pdc/index.php/Main/ProportionalIntegralControl, 2025.

[8] R. E. Precup and H. Hellendoorn, "A survey on industrial applications of fuzzy control," Computers in Industry, vol. 62, no. 3, pp. 213–226, Apr. 2011.

[9] S. S. Ge, C. C. Hang, and T. Zhang, "A new PID controller design via LMI approach," IEEE Transactions on Automatic Control, vol. 48, no. 4, pp. 534-539, 2003.

[10] M. Sugeno and T. Yasukawa, "A fuzzy-logic-based approach to qualitative modeling," IEEE Transactions on Fuzzy Systems, vol. 1, no. 1, pp. 7-31, 1993.

[11] L. X. Wang, "Stable adaptive fuzzy control of nonlinear systems," IEEE Transactions on Fuzzy Systems, vol. 1, no. 2, pp. 146-155, 1993.

[12] E. H. Mamdani and S. Assilian, "An experiment in linguistic synthesis with a fuzzy logic controller," International Journal of Man-Machine Studies, vol. 7, no. 1, pp. 1-13, 1975.

[13] T. Takagi and M. Sugeno, "Fuzzy identification of systems and its applications to modeling and control," IEEE Transactions on Systems, Man, and Cybernetics, vol. SMC-15, no. 1, pp. 116-132, 1985.

[14] C. C. Lee, "Fuzzy logic in control systems: fuzzy logic controller—Part I & II," IEEE Transactions on Systems, Man, and Cybernetics, vol. 20, no. 2, pp. 404-435, 1990.

[15] M. J. Schindler and H. L. Trentelman, "Adaptive fuzzy control of nonlinear systems using a multilayer neural network," IEEE Transactions on Neural Networks, vol. 7, no. 4, pp. 845-859, 1996.

[16] S. J. Ovaska and O. Vainio, "A fuzzy logic controller with an improved transient performance," IEEE Transactions on Industrial Electronics, vol. 39, no. 6, pp. 552-559, 1992.

[17] K. Tanaka and H. O. Wang, "Fuzzy control systems design and analysis: a linear matrix inequality approach," John Wiley & Sons, 2004.

[18] H. B. Verbruggen, R. Babuska, and W. Pedrycz, "Fuzzy algorithms for control," European Journal of Control, vol. 1, no. 2, pp. 41-50, 1995.

[19] A. D. Luca and G. Ulivi, "Design of fuzzy controllers based on input-output mapping," IEEE Transactions on Systems, Man, and Cybernetics, vol. 24, no. 1, pp. 163-171, 1994.

[20] P. J. Antsaklis and K. M. Passino, "An introduction to intelligent and autonomous control," Springer Science & Business Media, 2013.

[21] Kothari DP, Nagrath IJ. "Electric machine". 4th ed. NewDelhi: Tata McGraw Hill; 2010.

[22] Aydogmus O, Talu MF. "Comparison of extended kalman and particle filter-based sensorless speed control". IEEE Trans Instrum Meas. 61(2):402–410, 2012.